

Satellite Attitude Control and Power Tracking with Energy/Momentum Wheels

Panagiotis Tsiotras* and Haijun Shen†

Georgia Institute of Technology, Atlanta, Georgia 30332-0150

and

Chris Hall‡

Virginia Polytechnic Institute and State University, Blacksburg, Virginia 24061-0203

A control law for an integrated power/attitude control system (IPACS) for a satellite is presented. Four or more energy/momentum wheels in an arbitrary noncoplanar configuration and a set of three thrusters are used to implement the torque inputs. The energy/momentum wheels are used as attitude-control actuators, as well as an energy storage mechanism, providing power to the spacecraft. In that respect, they can replace the currently used heavy chemical batteries. The thrusters are used to implement the torques for large and fast (slew) maneuvers during the attitude-initialization and target-acquisition phases and to implement the momentum management strategies. The energy/momentum wheels are used to provide the reference-tracking torques and the torques for spinning up or down the wheels for storing or releasing kinetic energy. The controller published in a previous work by the authors is adopted here for the attitude-tracking function of the wheels. Power tracking for charging and discharging the wheels is added to complete the IPACS framework. The torques applied by the energy/momentum wheels are decomposed into two spaces that are orthogonal to each other, with the attitude-control torques and power-tracking torques in each space. This control law can be easily incorporated in an IPACS system onboard a satellite. The possibility of the occurrence of singularities, in which no arbitrary energy profile can be tracked, is studied for a generic wheel cluster configuration. A standard momentum management scheme is considered to null the total angular momentum of the wheels so as to minimize the gyroscopic effects and prevent the singularity from occurring. A numerical example for a satellite in a low Earth near-polar orbit is provided to test the proposed IPACS algorithm. The satellite's boresight axis is required to track a ground station, and the satellite is required to rotate about its boresight axis so that the solar panel axis is perpendicular to the satellite-sun vector.

Introduction

MOST spacecraft use chemical batteries (usually NiCd or NiH₂) to store excess energy generated by the solar panels during periods of exposure to the sun.¹ During an eclipse, the batteries are used to provide power for the spacecraft subsystems. The batteries are recharged when the spacecraft is in the sunlight. The primary problem with this approach is the cycle life of batteries and the additional power system mass required for controlling the charging and discharging cycles. Chemical batteries have shallow discharge depth (approximately 20–30% of their rated energy-storage capacity), large weight, and require operation within strict temperature limits (at or below 20°C in a low-Earth orbit) that often drive the entire spacecraft thermal design.

An alternative to chemical batteries is the use of flywheels to store energy. The use of flywheels has the benefit of increased efficiency (up to 90% depth of discharge with essentially unlimited life), operation in a relatively hot (up to 40°C) environment, and the potential to combine the energy-storage and the attitude-control functions into a single device, thus increasing reliability and reducing overall weight and spacecraft size. This concept, termed the integrated power and attitude-control system (IPACS) has been studied since the 1960s, but it has been particularly popular since the 1980s. In fact, the use of flywheels instead of batteries to store energy on spacecraft was suggested as early as 1961 in the paper by Roes,² when a 17 W·h/kg composite flywheel spinning at

10,000–20,000 rpm on magnetic bearings was proposed. The configuration included two counterrotating flywheels, and the author did not mention the possibility of using the momentum for attitude control. However, because many spacecraft use flywheels (in the form of momentum wheels, control moment gyros, etc.) to control attitude, the integration of these two functions is naturally of great interest. Numerous studies of this integration have been conducted. Anderson and Keckler³ originated the term IPACS in 1973. A study by Cormack⁴ done for the Rockwell Corporation examined the use of an integrated IPACS. Keckler and Jacobs⁵ presented a description of the concept. Will et al.⁶ investigated the IPACS concept and performed simulations by using (linearized) equations of motion. Notti et al.⁷ performed an extensive systems study and investigated linear control laws for attitude control. Their study included trade studies on the use of momentum wheels, control moment gyros, and counterrotating pairs. NASA and Boeing also conducted separate studies on the IPACS concept.^{8,9} Anand et al.^{10,11} discussed the system design issues associated with using magnetic bearings, as did Downer et al.¹² Flatley¹³ studied a tetrahedron array of four momentum wheels and considered the issues associated with simultaneously torquing the wheels for attitude control and energy storage. Around the same time as Flatley, O'Dea et al.¹⁴ included simultaneous attitude determination in their study of a combined attitude, reference, and energy-storage (CARES) system, focusing on technology-related issues. Oglevie and Eisenhaure^{15,16} performed a system-level study of IPACSS. Reference 15 includes a substantial list of references to earlier work. Olmsted¹⁷ presented technology-related issues associated with a particular flywheel design. Optimal design criteria associated with an integrated attitude-control and energy-storage (ACES) system have been discussed by Studer and Rodriguez.¹⁸

Most of these previous investigations of the IPACS focus on general design issues. The exact nonlinear equations of motions are not considered even when the attitude-control results are provided. In this paper, the exact nonlinear equations of motion are used to design an attitude controller that tracks a reference attitude profile.

Received 14 October 1999; revision received 4 March 2000; accepted for publication 17 March 2000. Copyright © 2000 by the authors. Published by the American Institute of Aeronautics and Astronautics, Inc., with permission.

*Associate Professor, School of Aerospace Engineering; p.tsiotras@ae.gatech.edu. Senior Member AIAA.

†Graduate Student, School of Aerospace Engineering; gt7318d@prism.gatech.edu. Student Member AIAA.

‡Associate Professor, Department of Aerospace and Ocean Engineering; chall@aoe.vt.edu. Associate Fellow AIAA.

The wheel-control torque space is decomposed into two spaces that are orthogonal to each other. The attitude-control torques lie in one of these two spaces, and the torques in the other space are used to spin up or down the energy/momentum wheels to store or extract kinetic energy. In the following sections, the system model is given first, then the reference attitude and energy/momentum-wheel power-tracking controllers are presented. A numerical example considering an iridium-type satellite¹⁹ in orbit is provided to illustrate the proposed IPACS methodology.

It should be pointed out that flywheels used in an IPACS typically rotate at much higher speeds than standard momentum wheels, as their operation is driven primarily by the energy-storage function rather than the attitude-control function. In this paper, we use the term energy/momentum wheels to emphasize this difference with commonly used momentum wheels.

System Model

Dynamics

Consider a rigid spacecraft with an N -wheel cluster installed to provide internal torques. Let \mathbf{B} denote the spacecraft body frame. Then the rotational equations of motion for the spacecraft can be expressed as

$$\dot{\mathbf{h}}_B = \mathbf{h}_B^\times \mathbf{J}^{-1} (\mathbf{h}_B - \mathbf{A} \mathbf{h}_a) + \mathbf{g}_e \quad (1a)$$

$$\dot{\mathbf{h}}_a = \mathbf{g}_a \quad (1b)$$

where \mathbf{h}_B is the angular-momentum vector of the spacecraft in the \mathbf{B} frame, given by

$$\mathbf{h}_B = \mathbf{J} \boldsymbol{\omega}_B + \mathbf{A} \mathbf{h}_a \quad (2)$$

where \mathbf{h}_a is the $N \times 1$ vector of the axial angular momenta of the wheels, $\boldsymbol{\omega}_B$ is the angular-velocity vector of the spacecraft in the \mathbf{B} frame, \mathbf{g}_e is the 3×1 vector of external torques, \mathbf{g}_a is the $N \times 1$ vector of the internal axial torques applied by the platform to the wheels, and \mathbf{A} is the $3 \times N$ matrix whose columns contain the axial unit vectors of the N energy/momentum wheels. \mathbf{J} is an inertial-like matrix defined as

$$\mathbf{J} = \mathbf{I} - \mathbf{A} \mathbf{I}_s \mathbf{A}^T \quad (3)$$

where \mathbf{I} is the moment of inertia of the spacecraft, including the wheels, and $\mathbf{I}_s = \text{diag}\{\mathbf{I}_{s1}, \mathbf{I}_{s2}, \dots, \mathbf{I}_{sN}\}$ is a diagonal matrix with the axial moments of inertia of the wheels.

The axial angular-momentum vector of the wheels can be written as

$$\mathbf{h}_a = \mathbf{I}_s \mathbf{A}^T \boldsymbol{\omega}_B + \mathbf{I}_s \boldsymbol{\omega}_s \quad (4)$$

where $\boldsymbol{\omega}_s = (\omega_{s1}, \omega_{s2}, \dots, \omega_{sN})^T$ is an $N \times 1$ vector denoting the axial angular velocity of the energy/momentum wheels with respect to the spacecraft. We denote the total axial angular velocity of the wheels relative to the inertial frame as $\boldsymbol{\omega}_c = (\omega_{c1}, \omega_{c2}, \dots, \omega_{cN})^T$. Using this notation, we can write Eq. (4) as

$$\mathbf{h}_a = \mathbf{I}_s \boldsymbol{\omega}_c \quad (5)$$

where $\boldsymbol{\omega}_c = \boldsymbol{\omega}_s + \mathbf{A}^T \boldsymbol{\omega}_B$. Note that because typically the wheels spin at a much higher speed than the spacecraft itself, $\boldsymbol{\omega}_s \gg \boldsymbol{\omega}_B$ and we have that $\boldsymbol{\omega}_c \approx \boldsymbol{\omega}_s$.

In Eq. (1) the external torques are assumed to include the control torque that is due to thruster firing, the gravity gradient torque, and the other disturbance torques, i.e.,

$$\mathbf{g}_e = \mathbf{g}_t + \mathbf{g}_g + \mathbf{g}_d \quad (6)$$

where the subscripts t , g , and d denote the thruster, gravity gradient, and disturbance, respectively. The gravity gradient torque is given by²⁰

$$\mathbf{g}_g = (3\mu / R_c^3) \hat{\mathbf{e}}_3^\times \mathbf{I} \hat{\mathbf{e}}_3 \quad (7)$$

where $\hat{\mathbf{e}}_3$ is the unit vector $-\mathbf{r}_c / R_c$ [the same as $\hat{\mathbf{z}}_l$, the z axis of the local-vertical local-horizontal (LVLH) frame, shown in Fig. 1]

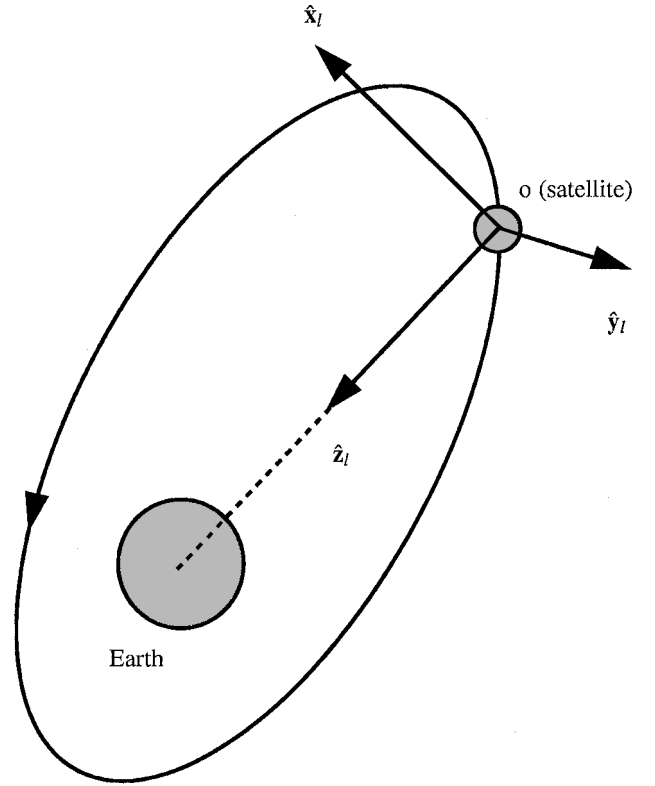


Fig. 1 LVLH frame.

expressed in the body frame, \mathbf{r}_c is the vector from the Earth center to the spacecraft center of mass with $R_c = |\mathbf{r}_c|$, and $\mu = 3.986005 \times 10^5 \text{ km}^3 \text{ s}^{-2}$ is the constant gravitational parameter. It should be pointed out that although we restrict the discussion to external control torques that are due to thruster firing, our approach remains the same for other choices of actuators, such as magnetotorques, etc.

Kinematics

The so-called modified Rodrigues parameters (MRPs) given in Refs. 21 and 22 are chosen to describe the attitude kinematics error of the spacecraft. The MRPs are defined in terms of the Euler principal unit vector $\hat{\boldsymbol{\ell}}$ and angle ϕ by

$$\boldsymbol{\sigma} = \hat{\boldsymbol{\ell}} \tan(\phi/4) \quad (8)$$

The MRPs have the advantage of being well defined for the whole range for rotations, i.e., $\phi \in [0, 2\pi)$. The differential equation governing the kinematics in terms of the MRPs is given by²¹

$$\dot{\boldsymbol{\sigma}} = \mathbf{G}(\boldsymbol{\sigma}) \boldsymbol{\omega} \quad (9)$$

where

$$\mathbf{G}(\boldsymbol{\sigma}) = \frac{1}{2} \{ \mathbf{1} + \boldsymbol{\sigma}^\times + \boldsymbol{\sigma} \boldsymbol{\sigma}^T - [(1 + \boldsymbol{\sigma}^T \boldsymbol{\sigma})/2] \mathbf{1} \} \quad (10)$$

and $\mathbf{1}$ is the 3×3 identity matrix.

Tracking Controller

In one of our previous works,²³ three control laws were presented to track a reference attitude profile by using coordinated action of both thrusters and momentum wheels. Here we restate the controller II from Ref. 23 that will be used for attitude tracking. This control law assumes that the reference frame dynamics and kinematics are given by

$$\dot{\mathbf{h}}_R = \mathbf{h}_R^\times \mathbf{J}^{-1} \mathbf{h}_R + \mathbf{g}_R \quad (11)$$

$$\dot{\boldsymbol{\sigma}}_R = \mathbf{G}(\boldsymbol{\sigma}_R) \boldsymbol{\omega}_R \quad (12)$$

where the subscript R stands for the reference frame to be tracked (referred to below as the desired or the target frame) and where $\mathbf{h}_R = \mathbf{J}\boldsymbol{\omega}_R$.

Given the reference attitude history to be tracked from Eqs. (11) and (12), the angular-velocity tracking error in the body frame is

$$\delta\boldsymbol{\omega} = \boldsymbol{\omega}_B - \mathbf{C}_R^B(\delta\boldsymbol{\sigma})\boldsymbol{\omega}_R \quad (13)$$

where $\mathbf{C}_R^B(\delta\boldsymbol{\sigma})$ is the rotation matrix from the reference frame R to the body frame B , and $\delta\boldsymbol{\sigma}$ is the MRP vector between the reference frame and the body frame, i.e.,

$$\mathbf{C}_R^B(\delta\boldsymbol{\sigma}) = \mathbf{C}_N^B[\mathbf{C}_N^R]^T \quad (14)$$

and the attitude error satisfies the following differential equation:

$$\delta\dot{\boldsymbol{\sigma}} = \mathbf{G}(\delta\boldsymbol{\sigma})\delta\boldsymbol{\omega} \quad (15)$$

A feedback control law to render $\delta\boldsymbol{\omega} \rightarrow 0$ and $\delta\boldsymbol{\sigma} \rightarrow 0$ is found with the following Lyapunov function:

$$V = \frac{1}{2}\delta\boldsymbol{\omega}^T \mathbf{J}^{-1}\delta\boldsymbol{\omega} + 2k_2 \ell_n(1 + \delta\boldsymbol{\sigma}^T \delta\boldsymbol{\sigma}) \quad (16)$$

where $k_2 > 0$. This function is positive definite and radially unbounded²¹ in terms of the tracking errors $\delta\boldsymbol{\omega}$ and $\delta\boldsymbol{\sigma}$. Taking the derivative of V and using Eqs. (13) and (15) yields the time derivative of V in terms of $\boldsymbol{\omega}_B$ and $\boldsymbol{\omega}_R$ and the tracking error $\delta\boldsymbol{\omega}$ and $\delta\boldsymbol{\sigma}$, i.e.,

$$\begin{aligned} \dot{V} = & \delta\boldsymbol{\omega}^T [\mathbf{h}_B^{\times} \mathbf{J}^{-1}(\mathbf{h}_B - \mathbf{A}\mathbf{h}_a) + \mathbf{g}_t + \mathbf{g}_g - \mathbf{J}\boldsymbol{\omega}_B^{\times} \delta\boldsymbol{\omega} \\ & - \mathbf{J}\mathbf{C}_R^B(\delta\boldsymbol{\sigma})\mathbf{J}^{-1}\mathbf{h}_R^{\times}\mathbf{J}^{-1}\mathbf{h}_R - \mathbf{J}\mathbf{C}_R^B(\delta\boldsymbol{\sigma})\mathbf{J}^{-1}\mathbf{g}_R - \mathbf{A}\mathbf{g}_a + k_2\delta\boldsymbol{\sigma}] \end{aligned} \quad (17)$$

The external torque \mathbf{g}_t is typically chosen to effect a desired large-angle attitude correction, whereas the internal torques \mathbf{g}_a are chosen to eliminate errors. For any external torque, if we select the internal torques such that

$$\begin{aligned} \mathbf{A}\mathbf{g}_a = & \mathbf{h}_B^{\times} \mathbf{J}^{-1}(\mathbf{h}_B - \mathbf{A}\mathbf{h}_a) + \mathbf{g}_t + \mathbf{g}_g - \mathbf{J}\boldsymbol{\omega}_B^{\times} \delta\boldsymbol{\omega} \\ & - \mathbf{J}\mathbf{C}_R^B(\delta\boldsymbol{\sigma})\mathbf{J}^{-1}\mathbf{h}_R^{\times}\mathbf{J}^{-1}\mathbf{h}_R - \mathbf{J}\mathbf{C}_R^B(\delta\boldsymbol{\sigma})\mathbf{J}^{-1}\mathbf{g}_R + k_1\delta\boldsymbol{\omega} + k_2\delta\boldsymbol{\sigma} \end{aligned} \quad (18)$$

with $k_1 > 0$, the derivative of the Lyapunov function is

$$\dot{V} = -k_1\delta\boldsymbol{\omega}^T \delta\boldsymbol{\omega} \leq 0 \quad (19)$$

As shown in Ref. 23, the tracking error system is asymptotically stable, i.e., $\boldsymbol{\omega}_B \rightarrow \boldsymbol{\omega}_R$ and $\boldsymbol{\sigma}_B \rightarrow \boldsymbol{\sigma}_R$ as $t \rightarrow \infty$.

Equation (18) allows for a variety of different control actions. In particular, once the thruster control action \mathbf{g}_t has been chosen, the energy/momentum-wheel action is computed directly from Eq. (18). Later on, we will use this equation to design control laws during two different phases of the satellite operation, namely the target-acquisition (attitude-initialization) phase and the attitude/power-tracking phase. We also point out that in the absence of initial errors [$\delta\boldsymbol{\omega}(0) = \delta\boldsymbol{\sigma}(0) = 0$] and for initial wheel axial momentum zero [$\mathbf{h}_a(0) = 0$], Eq. (18) reduces to $\mathbf{A}\mathbf{g}_a = 0$ and $\mathbf{g}_t = \mathbf{g}_R - \mathbf{g}_g$.

Given the torque action \mathbf{g}_t , we denote the right-hand side of Eq. (18) by \mathbf{f} . The internal torque provided by the wheels, \mathbf{g}_a , is given by the solution of the linear system $\mathbf{A}\mathbf{g}_a = \mathbf{f}$. If $N < 3$, this system is overdetermined and a solution may not exist; if $N = 3$ (and for noncoplanar wheels), the solution is uniquely determined; and if $N > 3$, the system is underdetermined and there exist an infinite number of solutions. In particular, in the latter case every solution has the form $\mathbf{g}_a = \mathbf{g}_r + \mathbf{g}_n$, where \mathbf{g}_r belongs to the range space $\mathcal{R}(A^T)$ of the matrix A^T and \mathbf{g}_n belongs to the null space $\mathcal{N}(A)$ of the matrix A .

It is seen that \mathbf{g}_n does not contribute to the attitude control input as $\mathbf{A}\mathbf{g}_n = 0$. One can always choose the torque \mathbf{g}_r to fulfill the equation $\mathbf{A}\mathbf{g}_r = \mathbf{f}$ and subsequently use \mathbf{g}_n to perform power/energy-storage management.²⁴ Note that this approach can be implemented as long as $\mathcal{N}(A)$ has nonzero dimension, which is always true for a cluster with more than three noncoplanar wheels.

In the following section, we consider a general momentum-wheel cluster and construct the torques in the null space of A so as not to disturb the attitude-control operation of the spacecraft and to track a desired power profile. In other words, the power- and the attitude-tracking operations are performed simultaneously and independently of one another. Power-tracking objectives do not interfere with attitude-tracking objectives and vice versa. We insist on this separation of objectives as it is unlikely that any IPACS that compromises either power or attitude-control requirement will be acceptable for use in routine spacecraft operations.

Power Tracking

As shown in the preceding section, the energy/momentum-wheel torque required for controlling the attitude is given by an expression of the form

$$\mathbf{A}\mathbf{g}_a = \mathbf{f} \quad (20)$$

where \mathbf{f} is the 3×1 required torque vector. The general solution for \mathbf{g}_a is given by

$$\mathbf{g}_a = \mathbf{A}^+ \mathbf{f} + \mathbf{g}_n \quad (21)$$

where $\mathbf{A}^+ = \mathbf{A}^T(\mathbf{A}\mathbf{A}^T)^{-1}$ is the projection operator on the range of A^T , and thus $\mathbf{A}^+ \mathbf{f} = \mathbf{g}_r \in \mathcal{R}(A^T)$, and where $\mathbf{g}_n \in \mathcal{N}(A)$, i.e.,

$$\mathbf{A}\mathbf{g}_n = 0 \quad (22)$$

Note that $\mathbf{A}\mathbf{g}_a = \mathbf{A}(\mathbf{A}^+ \mathbf{f} + \mathbf{g}_n) = \mathbf{f}$, so \mathbf{g}_n does not affect the spacecraft motion.

The total kinetic energy stored in the wheels is

$$T = \frac{1}{2}\boldsymbol{\omega}_c^T \mathbf{I}_s \boldsymbol{\omega}_c \quad (23)$$

The power (rate of change of the energy) is given by

$$\frac{dT}{dt} = P = \boldsymbol{\omega}_c^T \mathbf{I}_s \dot{\boldsymbol{\omega}}_c \quad (24)$$

The objective here is to find a controller \mathbf{g}_n in the null space of A to provide the required power function $P(t)$. Equation (5) implies that $\mathbf{g}_a = \mathbf{h}_a = \mathbf{I}_s \dot{\boldsymbol{\omega}}_c$, so from Eq. (24) we have

$$\boldsymbol{\omega}_c^T \mathbf{g}_a = P \quad (25)$$

Therefore, simultaneous attitude control and power management require a control torque vector \mathbf{g}_a that satisfies the following set of linear equations:

$$\begin{pmatrix} \mathbf{A} \\ \boldsymbol{\omega}_c^T \end{pmatrix} \mathbf{g}_a = \begin{pmatrix} \mathbf{f} \\ P \end{pmatrix} \quad (26)$$

From Eq. (21), we have that the torque \mathbf{g}_n in the null space of A has to satisfy

$$\boldsymbol{\omega}_c^T (\mathbf{A}^+ \mathbf{f} + \mathbf{g}_n) = P \quad (27)$$

or let the modified power $P_m = P - \boldsymbol{\omega}_c^T \mathbf{A}^+ \mathbf{f}$,

$$\boldsymbol{\omega}_c^T \mathbf{g}_n = P_m \quad (28)$$

Because $\mathbf{g}_n \in \mathcal{N}(A)$, there always exists a vector $\boldsymbol{\nu} \in \mathbb{R}^N$ such that

$$\mathbf{g}_n = \mathcal{P}_N \boldsymbol{\nu} \quad (29)$$

where $\mathcal{P}_N = \mathbf{1}_N - \mathbf{A}^T(\mathbf{A}\mathbf{A}^T)^{-1}\mathbf{A}$ is the (orthogonal) projection on $\mathcal{N}(A)$. Thus we have $\boldsymbol{\omega}_c^T \mathcal{P}_N \boldsymbol{\nu} = P_m$, to which a minimum norm solution is given by

$$\boldsymbol{\nu} = \mathcal{P}_N \boldsymbol{\omega}_c (\boldsymbol{\omega}_c^T \mathcal{P}_N \boldsymbol{\omega}_c)^{-1} P_m \quad (30)$$

and the energy management torque \mathbf{g}_n can then be chosen as

$$\mathbf{g}_n = \mathcal{P}_N \boldsymbol{\omega}_c (\boldsymbol{\omega}_c^T \mathcal{P}_N \boldsymbol{\omega}_c)^{-1} P_m \quad (31)$$

A solution of Eq. (31) exists as long as $\mathcal{P}_N \omega_c \neq 0$. This implies that either $\omega_c \neq 0$ or that $\omega_c \notin \mathcal{N}(A)^\perp = \mathcal{R}(A^T)$. The last requirement is also evident from Eq. (26), in which the matrix on the left-hand side does not have full row rank if $\omega_c \in \mathcal{R}(A^T)$.

It should be pointed out that, for satellite applications, during sunlight the solar panels provide enough power for the spacecraft equipment, and the wheels spin up to absorb and store the excess energy. Because the sunlight period is longer than the eclipse period, tracking a specific power function is less significant during the sunlight than during the eclipse period, when the power is solely provided by spinning down the wheels. Some authors have therefore chosen to discard power tracking altogether and simply spin up the wheels during sunlight to store the excess energy. This is the approach used, for example, in Ref. 13. On the contrary, unloading of the wheels during the eclipse is more critical, because the wheel deceleration should be done at a certain rate in order to provide the necessary power to the spacecraft bus.

Singularity Avoidance and Momentum Management

So far, we have found a controller g_a that tracks desired power profiles while controlling the spacecraft attitude. In addition, as was mentioned already, from Eq. (28) we can see that if ω_c lies in the range space of A^T , then because g_n is in the null space of A , we have

$$\omega_c^T g_n = 0 \quad (32)$$

This case is termed as singular, which implies that the controller loses the capability of tracking an arbitrary power function, and from Eq. (27) the only power the wheels can supply is $\omega_c^T A^+ f$. However, the latter case is undesirable in many practical applications. For example, for a stabilized spacecraft when the torque f is small, the amount of supplied power can be less than the required power level during the singularity.

For a three-axis stabilized satellite, if the angular momenta of the wheels are not distributed such that the total angular momentum of the wheels stays close to zero, the gyroscopic effects will play a significant role, increasing the required torque for the attitude control. Hence, in the following, a momentum management scheme will be included such that the total angular momentum of the wheels will become zero when some external torques are applied to the spacecraft, when needed. It will be seen that this scheme will further reduce the occurrence of the singularity mentioned above.

The ideal purpose of the momentum management is to make the total angular momentum of the wheels zero or keep it within certain limits. Here it is assumed that zero total momentum is required, i.e., $A h_a = 0$, which implies that $h_a \in \mathcal{N}(A)$. For a cluster with identical wheels (the typical case), Eq. (5) implies that $\omega_c \in \mathcal{N}(A)$. Recall now that singularity occurs when $\omega_c \in \mathcal{R}(A^T)$. But $\mathcal{N}(A) = \mathcal{R}(A^T)^\perp$ and, after momentum management, the wheel angular-velocity vector is orthogonal to the singularity subspace $\mathcal{R}(A^T)$. The possibility of singularity has thus been reduced as much as possible. This does not, of course, include the case in which $\omega_c = 0$, which belongs to both $\mathcal{N}(A)$ and $\mathcal{R}(A^T)$. However, because for a safety margin the energy stored in the wheels must always exceed the minimum energy level necessary for the spacecraft operation, the all-zero wheel angular velocity can happen only during initial satellite deployment, when the wheels may be in a locked position. In this case, the wheel angular-velocity initialization is performed after the deployment. In doing so, a torque in the null space of A is applied to the wheels to accelerate the wheel angular velocities to their normal operation range.

A simple momentum management scheme is adopted from Ref. 25. The torque required for momentum management is

$$g_t = -k(Ah_a - Ah_{an}) \quad (33)$$

where h_{an} denotes the nominal angular-momentum vector of the wheels and $k > 0$ is a feedback control gain. For the purpose of momentum unloading and singularity avoidance here we choose $Ah_{an} = 0$.

Numerical Example

To demonstrate the aforementioned algorithm for the attitude- and power-tracking controller, the following numerical example has

Table 1 Iridium 25578 orbital elements

n , rev/day	14.57788549
M_0 , deg	234.7460
ω , deg	125.5766
Ω , deg	132.8782
i , deg	86.5318
e	0.00216220
Epoch	05/23/1999 00:16:12.24

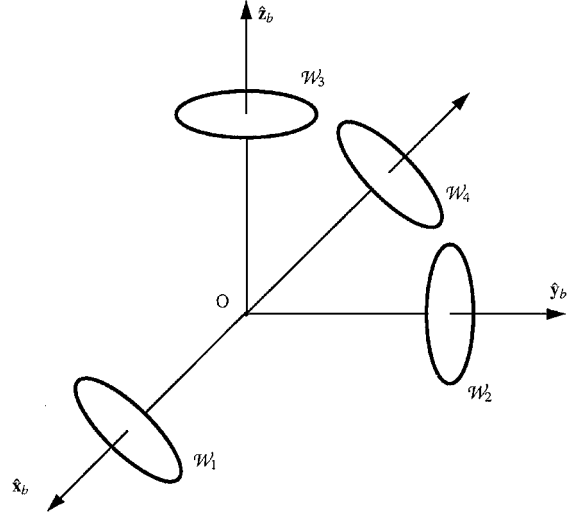


Fig. 2 Configuration of energy/momentum wheels.

been performed. A near-polar orbital satellite (orbital data chosen from the satellite Iridium 25578) is considered in this simulation.¹⁹ The orbital elements are shown in Table 1; n is the orbital frequency, M_0 is the mean anomaly at the epoch time, ω is the argument of perigee, Ω is the right ascension of the ascending node, i is the orbital inclination, and e is the eccentricity of the orbit. The satellite is assumed to have moment of inertia matrix in a principal axes system,

$$I = \begin{bmatrix} 200 & 0 & 0 \\ 0 & 200 & 0 \\ 0 & 0 & 175 \end{bmatrix} \text{ kg m}^2 \quad (34)$$

The four-wheel cluster, shown in Fig. 2, is chosen for this simulation. The wheels are assumed to have the same axial moments of inertia. The A matrix in this case is given by

$$A = \begin{bmatrix} 1 & 0 & 0 & \sqrt{3}/3 \\ 0 & 1 & 0 & \sqrt{3}/3 \\ 0 & 0 & 1 & \sqrt{3}/3 \end{bmatrix} \quad (35)$$

The normal power requirement of this satellite is 680 W. However, it is required to be able to provide an instantaneous peak power of 4 kW for up to 5 min. Considering the 34-min eclipse time and assuming that the 4-kW peak power lasts 5 min, we find that the wheels should store at least 0.72-kWh energy. With a 100% safety margin taken into account, the wheels are required to store 1.5-kWh energy when they are fully charged. Suppose that the nominal speed for the fourth wheel when the wheels are fully charged is -4000 rad/s ($-38,197$ rpm), and the speed for the other three is 2309.4 rad/s ($22,053$ rpm). These speeds render zero total angular momentum of the wheels. The energy and the wheel speed require that each wheel have an axial moment of inertia 0.338 kg m². Each energy/momentum wheel is assumed to provide a maximum torque of 1 N·m.

The disturbance torque that is due to aerodynamics, solar pressure, and other environmental factors is assumed to be²⁵

$$g_d = \begin{bmatrix} 4 \times 10^{-6} + 2 \times 10^{-6} \sin(nt) \\ 6 \times 10^{-6} + 3 \times 10^{-6} \sin(nt) \\ 3 \times 10^{-6} + 3 \times 10^{-6} \sin(nt) \end{bmatrix} \text{ N} \cdot \text{m} \quad (36)$$

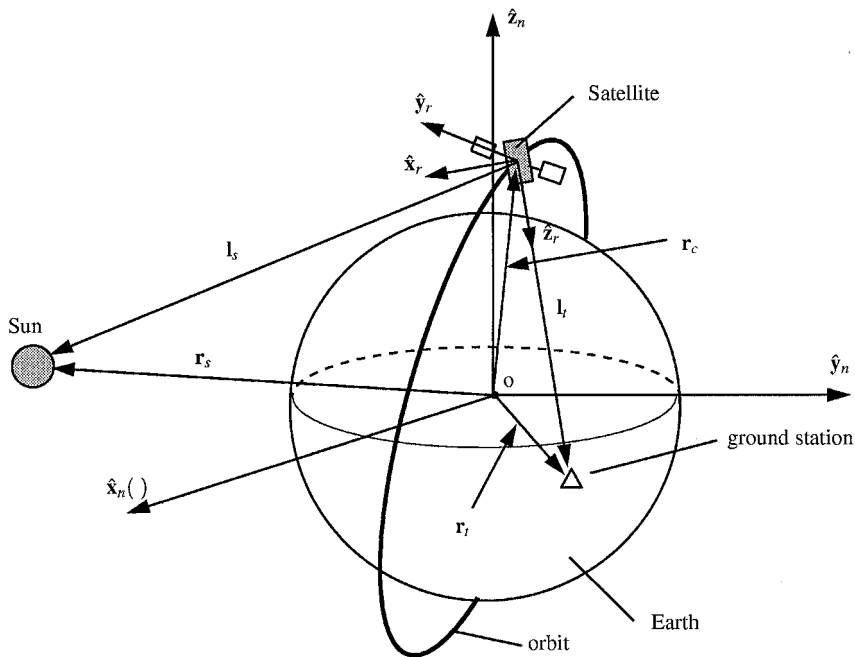


Fig. 3 Satellite mission illustration.

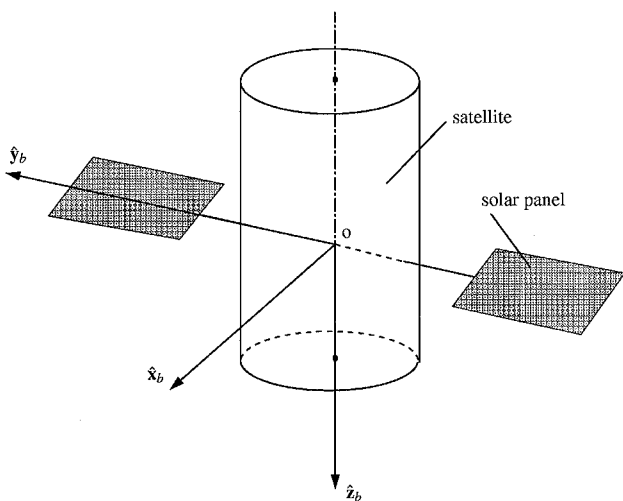


Fig. 4 Body frame of the satellite.

The satellite is required to perform sun and ground station tracking as follows. The symmetry axis should point to a ground station while the satellite is rotated by this axis such that the solar panel is perpendicular to the vector from the satellite to the sun. The ground station in this example is chosen to be Cape Canaveral (longitude 80.467°W, latitude 28.467°N). The sun and the ground station are assumed to be always available to the satellite. In the following subsection, we briefly describe the mission and the algorithm for obtaining the reference attitude maneuver history.

Mission Definition

The example is shown in Fig. 3. The inertial frame is chosen to be the J2000 geocentric inertial coordinate system, denoted by the subscript n . The vectors r_s , r_t , and r_c denote the positions of the sun, the ground station, and the satellite, respectively, and the vectors l_s and l_t denote the vectors from the satellite to the sun and the ground station. The following coordinate systems are used in the simulation besides the inertial frame, shown in Figs. 1 and 4. Hereafter, $\hat{(\cdot)}$ denotes a unit vector, and $\dot{(\cdot)}$ denotes the derivative with respect to time, taken in the inertial frame:

1) LVLH orbital frame, $o\hat{x}_l\hat{y}_l\hat{z}_l$, with the \hat{z}_l axis pointing toward the Earth center, the \hat{y}_l axis normal to the orbital plane, and the \hat{x}_l axis completing the orthogonal frame

2) body frame, $o\hat{x}_b\hat{y}_b\hat{z}_b$, with the \hat{z}_b axis along the boresight axis of the satellite and the \hat{y}_b axis pointing along the solar panels.

The mission requires that at each moment along the orbit, the \hat{z}_b axis should track the ground station, i.e., \hat{z}_b tracks the unit vector along l_t . In addition, the satellite should also track an attitude such that the \hat{y}_b axis is perpendicular to l_s .

Computing the Reference Attitude Profile

The satellite orbit is propagated by the orbit generator given in Ref. 26. From this, we know r_c , \dot{r}_c , and \ddot{r}_c in the inertial frame at any time. The sun position (r_s), velocity, (\dot{r}_s), and acceleration (\ddot{r}_s) in the inertial frame are computed by the algorithm given in Ref. 27. We can compute the position (r_t), velocity (\dot{r}_t), and acceleration (\ddot{r}_t) of the ground station in the inertial frame by converting the Universal Time (UT) into Greenwich Sidereal Time²⁶ (GST). From these, we know that

$$l_s = r_s - r_c, \quad \dot{l}_s = \dot{r}_s - \dot{r}_c, \quad \ddot{l}_s = \ddot{r}_s - \ddot{r}_c \quad (37a)$$

$$l_t = r_t - r_c, \quad \dot{l}_t = \dot{r}_t - \dot{r}_c, \quad \ddot{l}_t = \ddot{r}_t - \ddot{r}_c \quad (37b)$$

In the following subsection, the attitude, angular velocity, and angular acceleration of the reference frame, which are the desired attitude, angular velocity, and angular acceleration for the body frame, will be computed. The desired, or target, reference frame is denoted by $o\hat{x}_r\hat{y}_r\hat{z}_r$ and is shown in Fig. 3.

Attitude Reference

The rotation matrix C_N^L from the inertial frame to the LVLH frame can be readily computed by the orbital elements. Once the LVLH frame is known, we can write

$$l_t = (l_t \cdot \hat{x}_l)\hat{x}_l + (l_t \cdot \hat{y}_l)\hat{y}_l + (l_t \cdot \hat{z}_l)\hat{z}_l \quad (38)$$

so that

$$\hat{z}_r = [(l_t \cdot \hat{x}_l)\hat{x}_l + (l_t \cdot \hat{y}_l)\hat{y}_l + (l_t \cdot \hat{z}_l)\hat{z}_l] / \ell_t \quad (39)$$

where $\ell_t = \ell_t \hat{l}_t$. Because the \hat{y}_r axis is perpendicular to l_s and \hat{z}_r , it can be computed by

$$\hat{y}_r = \frac{\hat{z}_r \times \hat{l}_s}{|\hat{z}_r \times \hat{l}_s|} \quad (40)$$

and the \hat{x}_r axis is then given by

$$\hat{x}_r = \hat{y}_r \times \hat{z}_r \quad (41)$$

From the unit vectors \hat{x}_r , \hat{y}_r , and \hat{z}_r we can compute C_N^R , the rotation matrix from the inertial frame to the target reference frame. The value of $\eta_s = \hat{l}_s \cdot \hat{y}_b$ is used as a condition for sun tracking, i.e., $\eta_s = 0$ implies that the sun is being tracked. In addition, the value $\eta_t = |\hat{l}_t \times \hat{z}_b|$ is used as a condition for ground station tracking, i.e., $\eta_t = 0$ implies that the ground station is being tracked.

Angular-Velocity and the Angular-Acceleration References

We proceed to compute the angular velocity of the reference frame with respect to the inertial frame expressed in the target reference frame, $\omega_R = [\omega_{rx}, \omega_{ry}, \omega_{rz}]^T$. The algorithm for computing ω_{rx} and ω_{ry} can be found in Ref. 28.

The derivative of the vector l_t in the inertial frame can be written in the desired reference frame as

$$l_t = (l_t \cdot \hat{x}_r)\hat{x}_r + (l_t \cdot \hat{y}_r)\hat{y}_r + (l_t \cdot \hat{z}_r)\hat{z}_r \quad (42)$$

Notice that l_t can also be written as

$$l_t = \frac{{}^R d l_t}{dt} + \omega_R \times l_t = \frac{{}^R d l_t}{dt} + \omega_R \times (\mathcal{L}_t \hat{z}_r) \quad (43)$$

where ${}^R d l_t / dt$ is the derivative of l_t taken in the target reference frame. A comparison of Eqs. (42) and (43) then yields

$$\omega_{rx} = -l_t \cdot \hat{y}_r / \ell_t \quad (44a)$$

$$\omega_{ry} = l_t \cdot \hat{x}_r / \ell_t \quad (44b)$$

$$\frac{d {}^R l_t}{dt} = l_t \cdot \hat{z}_r \quad (44c)$$

Because $\hat{y}_r \cdot \hat{l}_s = 0$, its time derivative is

$$\dot{\hat{y}}_r \cdot \hat{l}_s + \hat{y}_r \cdot \dot{\hat{l}}_s = 0 \quad (45)$$

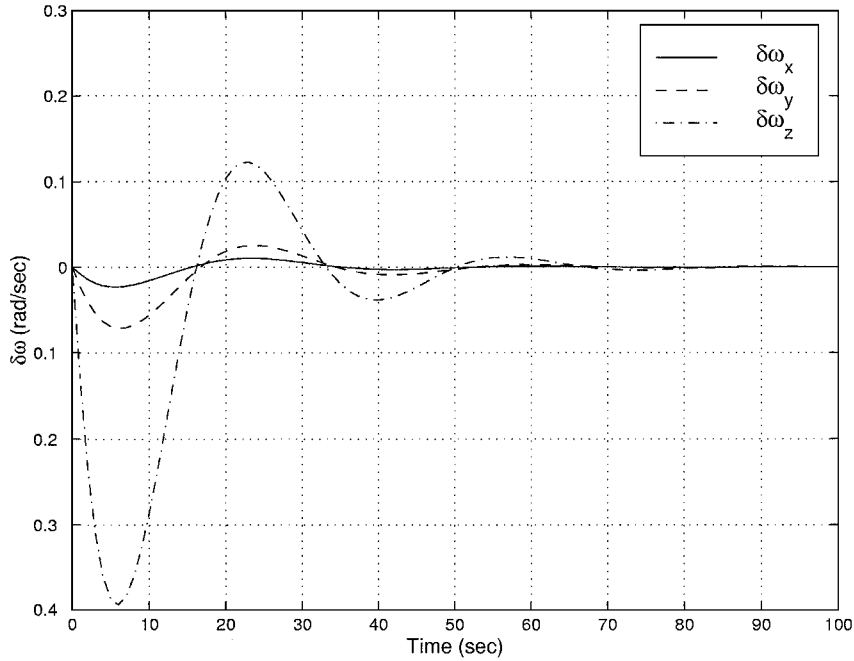


Fig. 5 Error in angular velocity of the satellite during target acquisition.

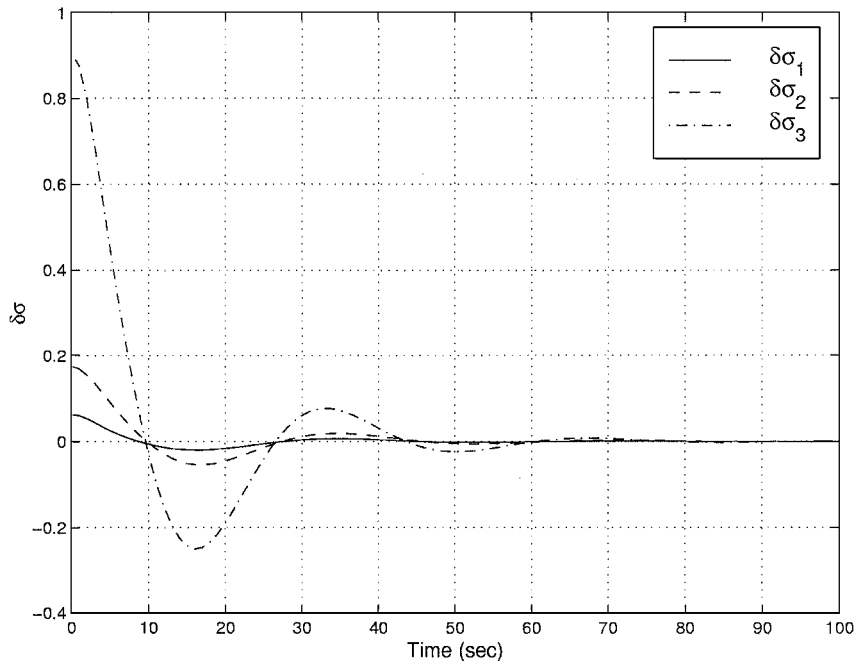


Fig. 6 Attitude error during target acquisition.

Expanding the derivative terms in the above equation, we end up with

$$\omega_{rz} = \frac{\omega_{rx} \mathbf{l}_s \cdot \hat{\mathbf{z}}_r + \mathbf{y}_r \cdot \dot{\mathbf{l}}_s}{\mathbf{l}_s \cdot \hat{\mathbf{x}}_r} \quad (46)$$

We can obtain the angular-acceleration vector $\dot{\boldsymbol{\omega}}_R = (\dot{\omega}_{rx}, \dot{\omega}_{ry}, \dot{\omega}_{rz})^T$ by taking the derivatives of ω_{rx} , ω_{ry} , and ω_{rz} . By doing so, we get

$$\dot{\omega}_{rx} = -(\dot{\mathbf{l}}_r \cdot \mathbf{y}_r + 2\omega_{rx} \ell_r) / \ell_r + \omega_{ry} \omega_{rz} \quad (47a)$$

$$\dot{\omega}_{ry} = (\dot{\mathbf{l}}_r \cdot \hat{\mathbf{x}}_r - 2\omega_{ry} \ell_r) / \ell_r - \omega_{rx} \omega_{rz} \quad (47b)$$

$$\dot{\omega}_{rz} = (M\dot{N} - N\dot{M}) / N^2 \quad (47c)$$

where

$$M = \omega_{rx} \mathbf{l}_s \cdot \hat{\mathbf{z}}_r + \mathbf{y}_r \cdot \dot{\mathbf{l}}_s \quad (48)$$

$$N = \mathbf{l}_s \cdot \hat{\mathbf{x}}_r \quad (49)$$

$$\begin{aligned} \dot{M} = & \omega_{rx} \dot{\mathbf{l}}_s \cdot \hat{\mathbf{z}}_r + \omega_{rx} \mathbf{l}_s \cdot \dot{\hat{\mathbf{z}}}_r + \dot{\omega}_{rx} \mathbf{l}_s \cdot (\boldsymbol{\omega}_R \times \hat{\mathbf{z}}_r) \\ & + \boldsymbol{\omega}_R \times \mathbf{y}_r \cdot \dot{\mathbf{l}}_s + \mathbf{y}_r \cdot \ddot{\mathbf{l}}_s \end{aligned} \quad (50)$$

$$\dot{N} = \dot{\mathbf{l}}_s \cdot \hat{\mathbf{x}}_r + \mathbf{l}_s \cdot (\boldsymbol{\omega}_R \times \hat{\mathbf{x}}_r) \quad (51)$$

Given $\boldsymbol{\omega}_R$ and $\dot{\boldsymbol{\omega}}_R$, we compute the reference torque \mathbf{g}_R from Eq. (11).

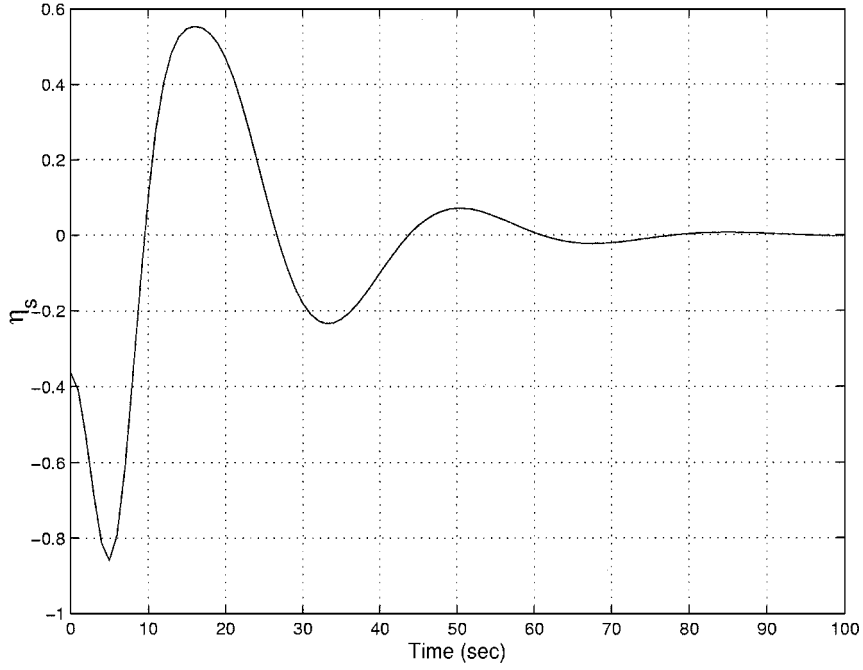


Fig. 7 Sun tracking condition during target acquisition ($\eta_s = \hat{\mathbf{l}}_s \cdot \hat{\mathbf{y}}_b$).

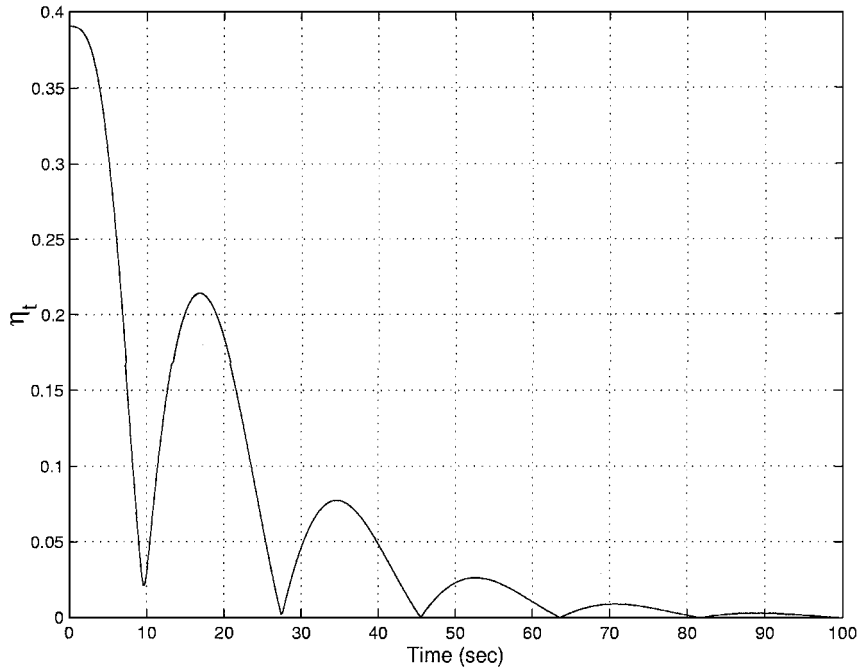


Fig. 8 Ground station tracking condition during target acquisition ($\eta_t = |\hat{\mathbf{l}}_t \times \hat{\mathbf{z}}_b|$).

Simulation Results

With the reference satellite attitude profile computed in the preceding section, we can apply the attitude- and power-tracking controller. Two simulations are conducted in sequence. First, a target-acquisition maneuver is performed with the thrusters, in which the satellite is maneuvered from the LVLH frame to the required sun and ground station tracking attitude. Then the attitude-control and energy-storage functions are switched on and the energy/momentum wheels are used to keep tracking the sun and the ground station. Here we assume that the wheels are spun up to their nominal angular velocities before deployment. This can be done with the power provided by the launch vehicle. If the wheels are in the locked position (not spinning) after separation, a constant torque $\mathbf{g}_a = [1/\sqrt{3} \ 1/\sqrt{3} \ 1/\sqrt{3} \ -1]^T$ (N·m), which is in the null space of the matrix \mathbf{A} , can be used to spin the wheels up without disturbing the satellite motion. The power for this initial spinup of the wheels

can be provided by the solar panels of the satellite. A problem may occur in case the solar panels do not face the sun at deployment. With body-mounted solar cells, it should not be a major concern, as some of the cells will be facing the sun any time the spacecraft is in the sunlight. Another approach is to have a primary (nonrechargeable) battery for the initial deployment/acquisition stage.

In the simulations, quaternions are used to describe the attitude from the inertial frame to the body and reference frames due to the large-angle orbital maneuver, and MRPs are used to describe the difference between the body and the reference frame. The results are presented in the following two subsections.

Target Acquisition

Before the satellite can be operated to track the sun and the ground station, target acquisition has to be performed so that the satellite is maneuvered to obtain the right attitude in order to start continuous

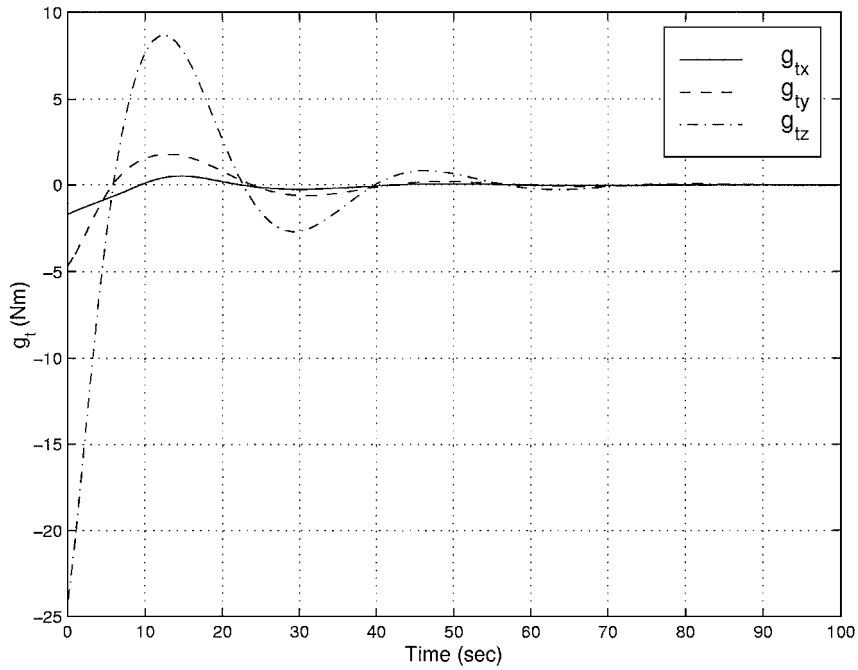


Fig. 9 Required thruster torque for the target acquisition ($g_a = 0$).

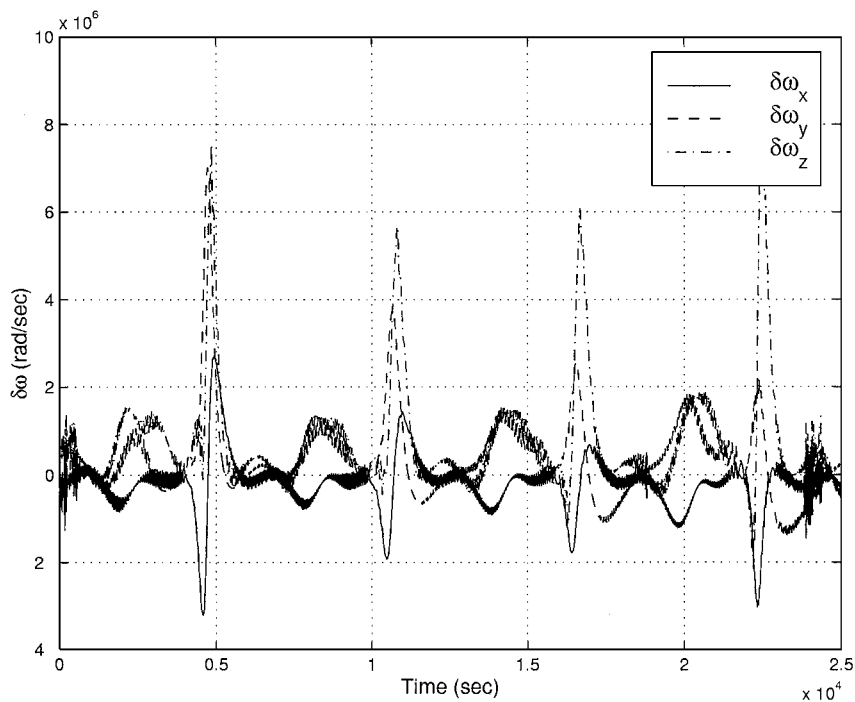


Fig. 10 Angular-velocity error during tracking.

tracking. The simulation starts with the satellite body frame aligned with the LVLH frame. Because this initial target-acquisition maneuver is usually a fast, large-angle (slew) maneuver and the wheels are of fairly low control authority (1 N · m in this example), external thrusters have to be used to issue the required torque, i.e., in Eq. (17), we choose

$$A\mathbf{g}_a = 0 \quad (52)$$

$$\mathbf{g}_t = -\mathbf{h}_B^{\times} \mathbf{J}^{-1} (\mathbf{h}_B - A\mathbf{h}_a) - \mathbf{g}_g + \mathbf{J} \omega_B^{\times} \delta\omega + \mathbf{J} \mathbf{C}_R^B(\delta\sigma) \mathbf{J}^{-1} \mathbf{h}_R^{\times} \mathbf{J}^{-1} \mathbf{h}_R + \mathbf{J} \mathbf{C}_R^B(\delta\sigma) \mathbf{J}^{-1} \mathbf{g}_R - k_1 \delta\omega - k_2 \delta\sigma \quad (53)$$

The controller gains are chosen as $k_1 = 24$ and $k_2 = 27$. Figure 5 shows the angular-velocity tracking error of the satellite, and Fig. 6 shows the quaternions of the body frame and the reference frame. It is seen that after ~ 70 s the satellite attitude tracks the refer-

ence. In Fig. 7 it is shown that the sun tracking condition value η_s goes to zero after ~ 90 s. In Fig. 8 it is shown that the ground station tracking condition value η_h goes to zero also after ~ 90 s. Figure 9 shows the torque required for performing the target-acquisition maneuver.

Continuous Tracking

After the satellite tracks the sun and the ground station, the energy/momentum-wheel attitude- and power-tracking control is switched on, so that the satellite will keep tracking the sun and the ground station. In this case, the wheels will provide both the target-tracking torques and the energy-storage torques. The thrusters will only be used to issue the necessary momentum management torque, i.e., in Eq. (17), we choose for every two orbits

$$\mathbf{g}_t = -k(\mathbf{A}\mathbf{h}_a - \mathbf{A}\mathbf{h}_{an}) \quad (54)$$

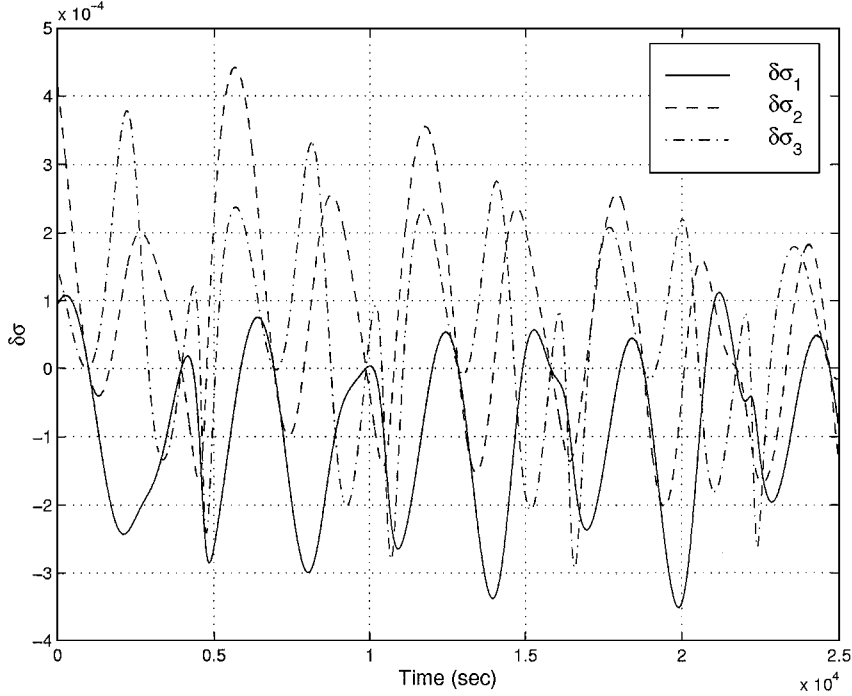


Fig. 11 Attitude error during tracking.

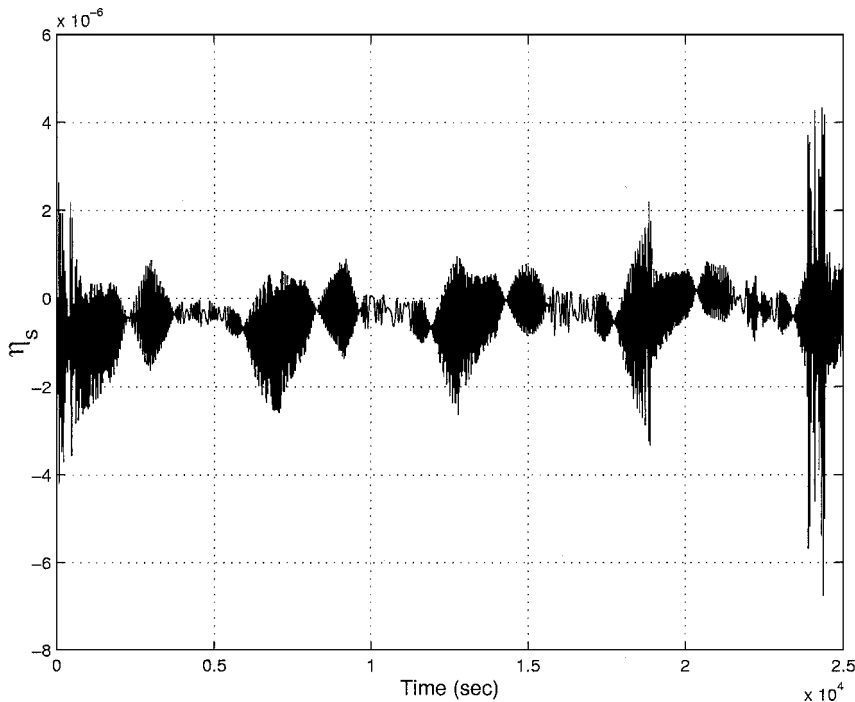


Fig. 12 Sun tracking condition during tracking ($\eta_s = \mathbf{l}_s \cdot \dot{\mathbf{y}}_b$).

$$\begin{aligned}
 \mathbf{A}g_a = & \mathbf{h}_B^\times \mathbf{J}^{-1} (\mathbf{h}_B - \mathbf{A}h_a) + \mathbf{g}_t + \mathbf{g}_g - \mathbf{J}\omega_B^\times \delta\omega \\
 & - \mathbf{J}C_R^B(\delta\sigma) \mathbf{J}^{-1} \mathbf{h}_R^\times \mathbf{J}^{-1} \mathbf{h}_R - \mathbf{J}C_R^B(\delta\sigma) \mathbf{J}^{-1} \mathbf{g}_R \\
 & + k_1 \delta\omega + k_2 \delta\sigma
 \end{aligned} \quad (55)$$

The simulation orbit starts from 02/23/99 07:59:32.28 and lasts for 25,000 s (approximately 4 orbits). The controller gains are chosen as $k_1 = 24$, $k_2 = 27$, and $k = 0.005$. During the eclipse, the nominal power requirement during eclipse is 680 W, with an additional requirement of 4-kW power for 5 min. During sunlight, the wheels are charged with a power level of 1 kW until the total energy stored in the wheels reaches 1.5 kWh. After the wheels are charged, the momentum management is switched on every two orbits. Figures 10 and 11 show the angular velocity and attitude error during tracking.

The angular-velocity errors are practically zero for the whole period of the maneuver. The largest errors occur at the times of the highest wheel momenta; compare with Fig. 15. The attitude error in Fig. 11 corresponds to a pointing error of less than 0.1 deg about all three axes. Figures 12 and 13 show that the sun and ground station tracking conditions are being satisfied. Figure 14 shows the power profile with the sunlight and eclipse indication, where sunlight is indicated by 1 and eclipse is indicated by -1 . The corresponding torque applied by the wheels is shown in Fig. 15, along with the total angular momentum of the wheels. As expected, the wheels charge during sunlight and discharge during the eclipse. Every two orbits (at approximately 0.6×10^4 and 1.8×10^4 s in Fig. 15) the total angular momentum of the wheels $\mathbf{A}h_a$ goes to zero because of proper momentum management. Finally, Fig. 16 shows the wheel speeds.

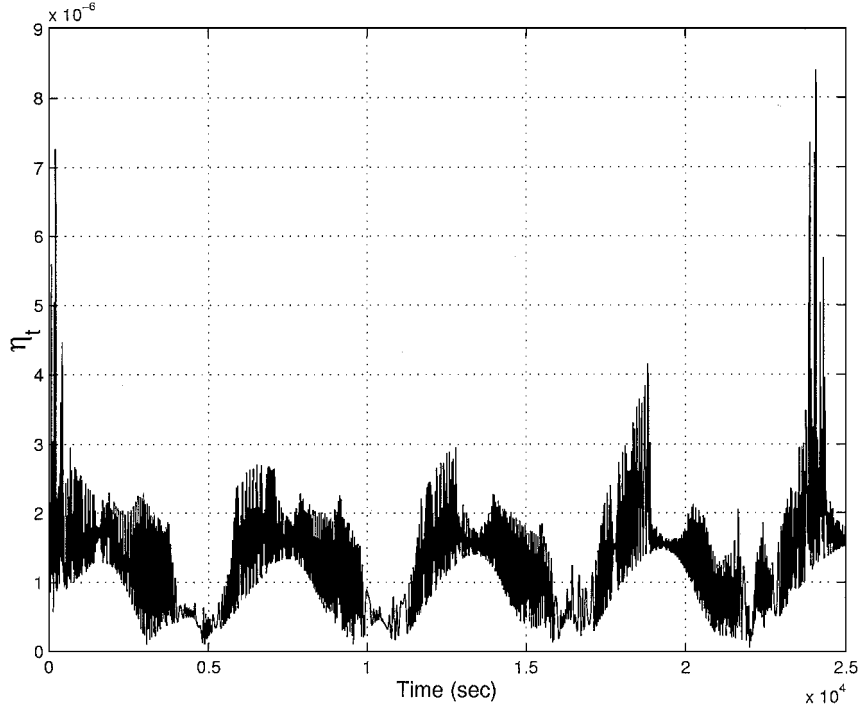


Fig. 13 Ground station tracking condition during tracking ($\eta_t = |l_t \times z_b|$).

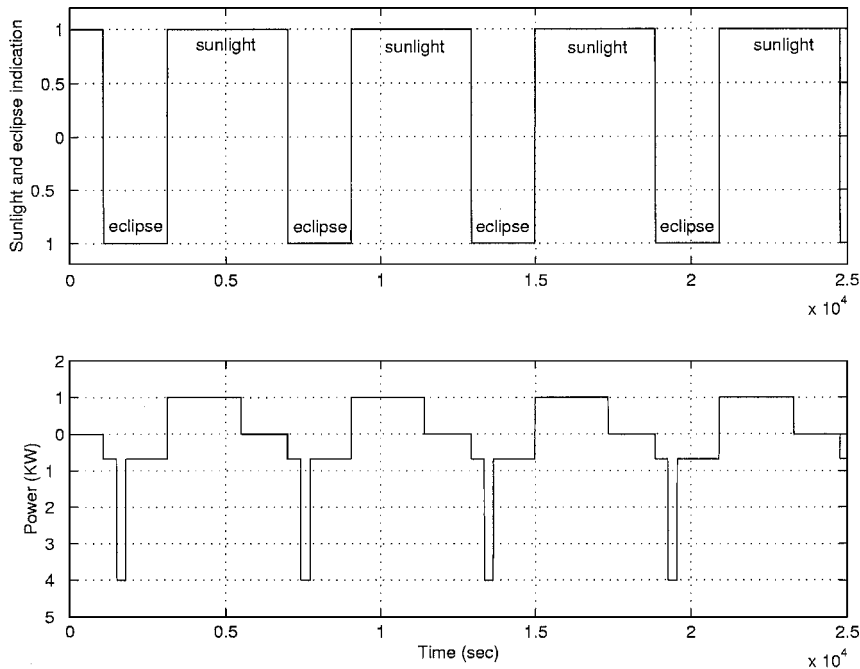


Fig. 14 Sunlight/eclipse indication and power profile.

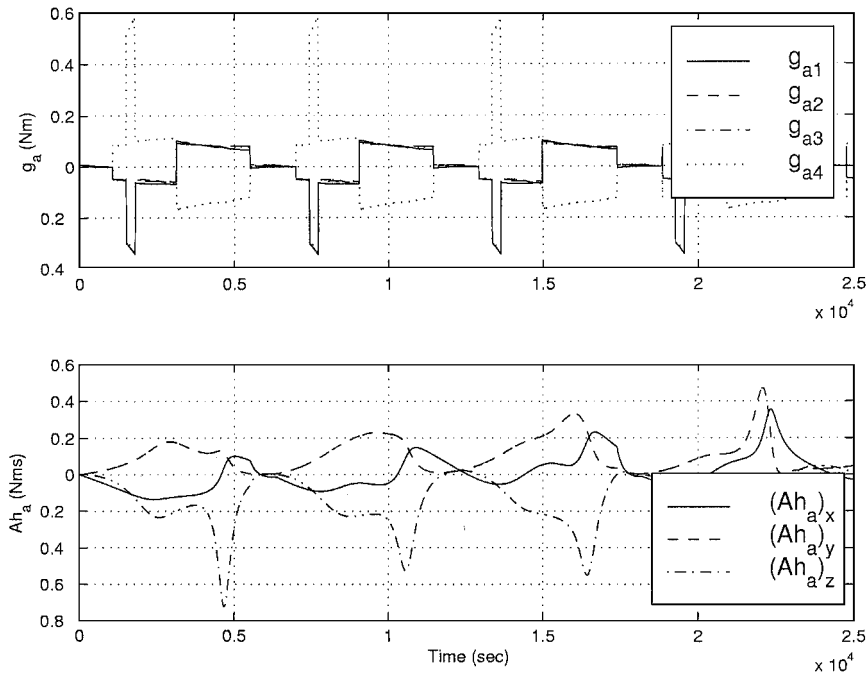


Fig. 15 Axial torques and the total angular momentum of the energy/momentum wheels.

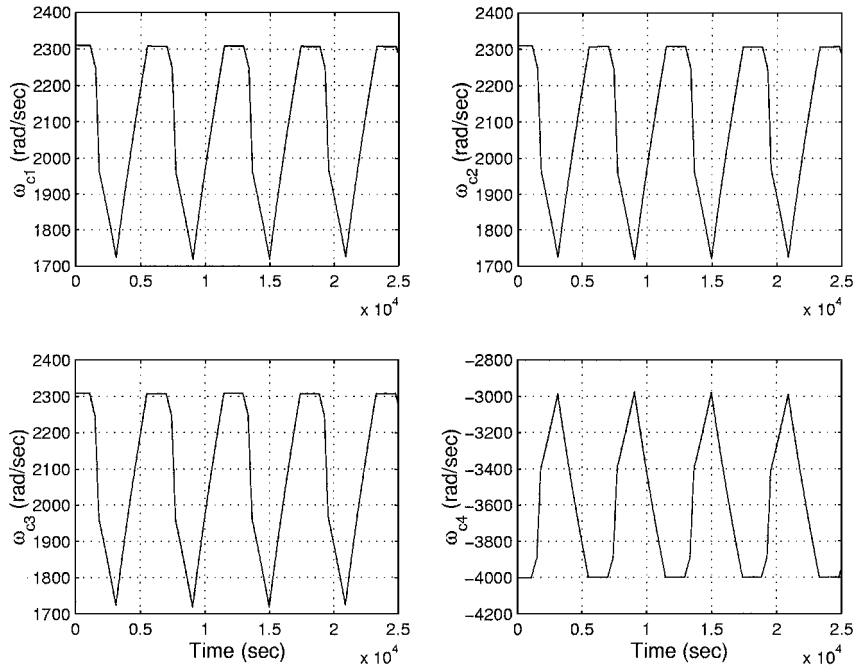


Fig. 16 Angular velocities of the energy/momentum wheels.

These plots indicate that there are no major theoretical problems in using a cluster of four or more energy/momentum wheels in a suitable geometric configuration to successfully control the attitude and power requirements of a satellite in a typical Earth orbit example. In reality, several issues need to be addressed before the implementation of such a control law for an IPACS. For instance, vibration suppression algorithms for high-speed flywheels, proper rotor sizing, and containment issues are of great interest in that respect. These and other similar issues are left for future investigation.

Conclusions

In this paper, we develop an algorithm for controlling the spacecraft attitude while simultaneously tracking a desired power profile by using a cluster of more than three noncoplanar energy/momentum wheels. The torque is decomposed into two perpendicular spaces. One is the null space of this matrix whose columns are the unit

vectors along the axes of each wheel. The torque in this space is used to track the required power level of the wheels, and the torque in the space perpendicular to the null space of this matrix is used to control the attitude of the satellite. The torque decomposition is based on solving a set of linear equations. Singularities may occur in case the coefficient matrix does not have full row rank. In this case, no arbitrary power profile can be tracked. A momentum management scheme is considered to null the total angular momentum of the wheels in order to minimize the gyroscopic effects and also prevent the occurrence of singularities. A numerical example based on a realistic example for an iridium-type satellite demonstrates the efficacy of the proposed algorithm.

References

¹Wertz, J., and Larson, W. (eds.), *Space Mission Analysis and Design*, Kluwer Academic, Boston, 1991, pp. 349–369.

- ²Roes, J. B., "An Electro-Mechanical Energy Storage System for Space Application," *Progress in Astronautics and Rocketry*, Vol. 3, Academic, New York, 1961, pp. 613–622.
- ³Anderson, W. W., and Keckler, C. R., "An Integrated Power/Attitude Control System (IPACS) for Space Application," *Proceedings of the 5th IFAC Symposium on Automatic Control in Space*, Pergamon, New York, 1973, pp. 81, 82.
- ⁴Cormack III, A., "Three Axis Flywheel Energy and Control Systems," NASA TN-73-G&C-8, 1973.
- ⁵Keckler, C. R., and Jacobs, K. L., "A Spacecraft Integrated Power/Attitude Control System," *Proceedings of the 9th Intersociety Energy Conversion Engineering Conference*, American Society of Mechanical Engineers, New York, 1974, pp. 20–25.
- ⁶Will, R. W., Keckler, C. R., and Jacobs, K. L., "Description and Simulation of an Integrated Power and Attitude Control System Concept for Space-Vehicle Application," NASA TN D-7459, 1974.
- ⁷Notti, J. E., Cormack III, A., Schmill, W. C., and Klein, W. J., "Integrated Power/Attitude Control System (IPACS) Study: Volume II—Conceptual Designs," NASA CR-2384, 1974.
- ⁸Rodriguez, G. E., Studer, P. A., and Baer, D. A., "Assessment of Flywheel Energy Storage for Spacecraft Power Systems," NASA TM-85061, 1983.
- ⁹Gross, S., "Study of Flywheel Energy Storage for Space Stations," NASA CR-171780, 1984.
- ¹⁰Anand, D., Kirk, J. A., and Frommer, D. A., "Design Considerations for Magnetically Suspended Flywheel Systems," *Proceedings of the 20th Intersociety Energy Conversion Engineering Conference*, Vol. 2, Society of Automotive Engineers, Warrendale, PA, 1985, pp. 449–453.
- ¹¹Anand, D., Kirk, J. A., Amood, R. B., Studer, P. A., and Rodriguez, G. E., "System Considerations for Magnetically Suspended Flywheel Systems," *Proceedings of the 21st Intersociety Energy Conversion Engineering Conference*, American Chemical Society, Washington, DC, Vol. 3, 1986, pp. 1829–1833.
- ¹²Downer, J., Eisenhaure, D., Hockney, R., Johnson, B., and O'Dea, S., "Magnetic Suspension Design Options for Satellite Attitude Control and Energy Storage," *Proceedings of the 20th Intersociety Energy Conversion Engineering Conference*, Society of Automotive Engineers, Warrendale, PA, Vol. 2, 1985, pp. 424–430.
- ¹³Flatley, T., "Tetrahedron Array of Reaction Wheels for Attitude Control and Energy Storage," *Proceedings of the 20th Intersociety Energy Conversion Engineering Conference*, Society of Automotive Engineers, Warrendale, PA, Vol. 2, 1985, pp. 2353–2360.
- ¹⁴O'Dea, S., Burdick, P., Downer, J., Eisenhaure, D., and Larkin, L., "Design and Development of a High Efficiency Effector for the Control of Attitude and Power in Space Systems," *Proceedings of the 20th Intersociety Energy Conversion Engineering Conference*, Society of Automotive Engineers, Warrendale, PA, Vol. 2, 1985, pp. 353–360.
- ¹⁵Oglevie, R. E., and Eisenhaure, D. B., "Advanced Integrated Power and Attitude Control System (IPACS) Technology," NASA CR-3912, Nov. 1985.
- ¹⁶Oglevie, R. E., and Eisenhaure, D. B., "Integrated Power and Attitude Control System (IPACS) Technology," *Proceedings of the 21st Intersociety Energy Conversion Engineering Conference*, American Chemical Society, Washington, DC, Vol. 3, 1986, pp. 1834–1837.
- ¹⁷Olmsted, D. R., "Feasibility of Flywheel Energy Storage in Spacecraft Applications," *Proceedings of the 20th Intersociety Energy Conversion Engineering Conference*, Society of Automotive Engineers, Warrendale, PA, Vol. 2, 1985, pp. 444–448.
- ¹⁸Studer, P., and Rodriguez, E., "High Speed Reaction Wheels for Satellite Attitude Control and Energy Storage," *Proceedings of the 20th Intersociety Energy Conversion Engineering Conference*, Vol. 2, Society of Automotive Engineers, Warrendale, PA, 1985, pp. 349–352.
- ¹⁹Fossa, C. E., Raines, R. A., Gunsch, G. H., and Temple, M. A., "An Overview of the IRIDIUM Low Earth Orbit (LEO) Satellite System," *Proceedings of the IEEE National Aerospace and Electronics Conference*, Inst. of Electrical and Electronics Engineers, Piscataway, NJ, 1998, pp. 152–159.
- ²⁰Hughes, P., *Spacecraft Attitude Dynamics*, Wiley, New York, 1986, pp. 233–248.
- ²¹Tsiotras, P., "Stabilization and Optimality Results for the Attitude Control Problem," *Journal of Guidance, Control, and Dynamics*, Vol. 19, No. 4, 1996, pp. 772–777.
- ²²Shuster, M. D., "A Survey of Attitude Representations," *Journal of the Astronautical Sciences*, Vol. 41, No. 4, 1993, pp. 439–517.
- ²³Hall, C., Tsiotras, P., and Shen, H., "Tracking Rigid Body Motion Using Thrusters and Reaction Wheels," AIAA Paper 98-4471, Aug. 1998.
- ²⁴Hall, C., "High-Speed Flywheels for Integrated Energy Storage and Attitude Control," *Proceedings of the American Control Conference*, Vol. 3, IEEE Publications, Piscataway, NJ, 1997, pp. 1894–1898.
- ²⁵Sidi, M., *Spacecraft Dynamics and Control, A Practical Engineering Approach*, Cambridge Univ. Press, New York, 1997, pp. 241, 242.
- ²⁶Wertz, J. (ed.), *Spacecraft Attitude Determination and Control*, Reidel, Boston, 1997, pp. 132–138.
- ²⁷Meeus, J., *Astronomical Algorithms*, Willmann-Bell, Richmond, VA, 1991, Chaps. 21, 24, 25, 31 and Appendices.
- ²⁸Hablani, H., "Design of a Payload Pointing Control system for Tracking Moving Objects," *Journal of Guidance, Control, and Dynamics*, Vol. 12, No. 3, 1989, pp. 365–374.